Anal. Chem. **2007,** *79,* 6650−6654

Homogeneous Detection of Nucleic Acids Based upon the Light Scattering Properties of Silver-Coated Nanoparticle Probes

Xiaoyang Xu, Dimitra G. Georganopoulou, Haley D. Hill, and Chad A. Mirkin*

Department of Chemistry and International Institute for Nanotechnology, Northwestern University, 2145 Sheridan Road, Evanston, Illinois 60208-3113

Herein we report the development of a simple, rapid, homogeneous, and sensitive detection system for DNA based on the scattering properties of silver-amplified gold nanoparticle probes. The assay uses DNA-functionalized magnetic particle probes that act as scavengers for target DNA, which can be collected via a magnetic field. Once the DNA targets are isolated from the initial sample, they are sandwiched via hybridization by a second set of probes. The latter probes are 13-nm gold nanoparticles modified with a different target complementary DNA. Excess probes are removed through repetitive washing steps. The gold particles are dispersed in solution by dehybridization, corresponding to an assumed 1:1 ratio with the target DNA. Electroless deposition of silver on the surface of the gold probes results in particle growth, which increases their scattering efficiency with time. The scattering efficiency and the extinction signatures of the particle sizes are monitored as a function of time and correlated with target concentration. The limit of detection for this novel assay was determined to be 10 fM.

There are now a variety of methods for detecting nucleic acids.[1] These include techniques based upon fluorescence,[2−5] radioactivity,[6] the quartz crystal microbalance,[7,8] Raman spectroscopy,[9] colorimetry,[10−12] and electrochemistry.[13,14] In most cases, molecular probes are used to label the target molecule of interest, in a manner that provides suitable readout. Recently, there has been significant interest in using nanoparticle probes as alternatives to molecular ones. Gold nanoparticles[15−19] and quantum dots[3,20] have been a major focus of study in this regard. Gold nanoparticles, in particular, when heavily modified with thiolated oligonucleotides, exhibit target binding properties that translate into selectivity advantages and catalytic properties that lead to sensitivity enhancement when compared to molecular probe analogues of the same sequence.[21,22] These types of probes have led to chip-based sandwich assays for DNA, which rely on the scattering,[23−25] absorbance,[11,15] conductivity,[26] or spectroscopic signatures[22] of the metal particle probes. Some of these assays now rival molecular fluorophore probe-based PCR assays in terms of sensitivity[27−29] and have been shown to be capable of identifying and differentiating single-nucleotide polymorphisms in genomic DNA targets without the need for enzymatic amplification.[30,31]

Relatively little has been done to evaluate the potential of using gold nanoparticle probes for homogeneous detection formats (i.e.,

* To whom correspondence should be addressed. E-mail: chadnano@northwestern.edu.

(1) Ramsey, J. M. *Nat. Biotechnol.* **1999**, *17*, 1061−1062.
(2) Zhao, X. J.; Tapec-Dytioco, R.; Tan, W. H. *J. Am. Chem. Soc.* **2003**, *125*, 11474−11475.
(3) Bruchez, M.; Moronne, M.; Gin, P.; Weiss, S.; Alivisatos, A. P. *Science* **1998**, *281*, 2013−2016.
(4) Han, M. Y.; Gao, X. H.; Su, J. Z.; Nie, S. *Nat. Biotechnol.* **2001**, *19*, 631−635.
(5) Heid, C. A.; Stevens, J.; Livak, K. J.; Williams, P. M. *Genome Res.* **1996**, *6*, 986−994.
(6) Jordan, B. R. *J. Biochem.* **1998**, *124*, 251−258.
(7) Patolsky, F.; Lichtenstein, A.; Willner, I. *J. Am. Chem. Soc.* **2000**, *122*, 418−419.
(8) Weizmann, Y.; Patolsky, F.; Willner, I. *Analyst* **2001**, *126*, 1502−1504.
(9) Cao, Y. W. C.; Jin, R. C.; Mirkin, C. A. *Science* **2002**, *297*, 1536−1540.
(10) Tizard, R.; Cate, R. L.; Ramachandran, K. L.; Wysk, M.; Voyta, J. C.; Murphy, O. J.; Bronstein, I. *Proc. Natl. Acad. Sci. U.S.A.* **1990**, *87*, 4514−4518.
(11) Elghanian, R.; Storhoff, J. J.; Mucic, R. C.; Letsinger, R. L.; Mirkin, C. A. *Science* **1997**, *277*, 1078−1081.
(12) Sato, K.; Hosokawa, K.; Maeda, M. *J. Am. Chem. Soc.* **2003**, *125*, 8102−8103.
(13) Drummond, T. G.; Hill, M. G.; Barton, J. K. *Nat. Biotechnol.* **2003**, *21*, 1192−1199.
(14) Wang, J. *Analyst* **2005**, *130*, 421−426.
(15) Mirkin, C. A.; Letsinger, R. L.; Mucic, R. C.; Storhoff, J. J. *Nature* **1996**, *382*, 607−609.
(16) Penn, S. G.; He, L.; Natan, M. J. *Curr. Opin. Chem. Biol.* **2003**, *7*, 609−615.
(17) Niemeyer, C. M. *Angew. Chem., Int. Ed.* **2001**, *40*, 4128−4158.
(18) Parak, W. J.; Gerion, D.; Pellegrino, T.; Zanchet, D.; Micheel, C.; Williams, S. C.; Boudreau, R.; Le Gros, M. A.; Larabell, C. A.; Alivisatos, A. P. *Nanotechnology* **2003**, *14*, R15−R27.
(19) Rosi, N. L.; Mirkin, C. A. *Chem. Rev.* **2005**, *105*, 1547−1562.
(20) Chan, W. C. W.; Nie, S. M. *Science* **1998**, *281*, 2016−2018.
(21) Lytton-Jean, A. K. R.; Mirkin, C. A. *J. Am. Chem. Soc.* **2005**, *127*, 12754−12755.
(22) Taton, T. A.; Mirkin, C. A.; Letsinger, R. L. *Science* **2000**, *289*, 1757−1760.
(23) Stimpson, D. I.; Hoijer, J. V.; Hsieh, W. T.; Jou, C.; Gordon, J.; Theriault, T.; Gamble, R.; Baldeschwieler, J. D. *Proc. Natl. Acad. Sci. U.S.A.* **1995**, *92*, 6379−6383.
(24) Yguerabide, J.; Yguerabide, E. E. *Anal. Biochem.* **1998**, *262*, 137−156.
(25) Yguerabide, J.; Yguerabide, E. E. *J. Cell. Biochem.* **2001**, 71−81.
(26) Park, S. J.; Taton, T. A.; Mirkin, C. A. *Science* **2002**, *295*, 1503−1506.
(27) Saiki, R. K.; Scharf, S.; Faloona, F.; Mullis, K. B.; Horn, G. T.; Erlich, H. A.; Arnheim, N. *Science* **1985**, *230*, 1350−1354.
(28) Kopp, M. U.; de Mello, A. J.; Manz, A. *Science* **1998**, *280*, 1046−1048.
(29) Makrigiorgos, G. M.; Chakrabarti, S.; Zhang, Y. Z.; Kaur, M.; Price, B. D. *Nat. Biotechnol.* **2002**, *20*, 936−939.
(30) Storhoff, J. J.; Marla, S. S.; Bao, P.; Hagenow, S.; Mehta, H.; Lucas, A.; Garimella, V.; Patno, T.; Buckingham, W.; Cork, W.; Muller, U. R. *Biosens. Bioelectron.* **2004**, *19*, 875−883.
(31) Storhoff, J. J.; Lucas, A. D.; Garimella, V.; Bao, Y. P.; Muller, U. R. *Nat. Biotechnol.* **2004**, *22*, 883−887.

10.1021/ac070867g CCC: $37.00
Published on Web 07/31/2007

Scheme 1. Homogeneous Detection of DNA[a]

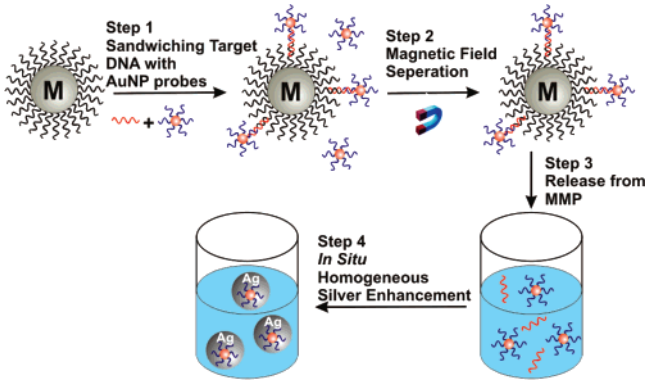

[a] Magnetic microparticle probes capture target DNA. Gold nanoparticle probes hybridize to a different portion of the target sequence. A bar magnet localizes the target probe sandwich complexes. Unbound gold particles are removed by washing. Dehybridization of the gold particles from the sandwich complex followed by silver deposition on the gold particles provides amplification and straightforward detection by the naked eye, and absorbance measurement or a light scatter measurement. Sequence information: Au NP, (5′-HS-$(CH_2)_6$-A_{10}-PEG_{18}-CTT GAC TTT GGG GAT TGT AGG-3′); DNA target, (5′-ATT TTC GGG TTT ATT ACA GG-PEG_{18}-CCT ACA ATC CCC AAA GTC AAG-3′); MMP, (5′- NH_2-$(CH_2)_6$-A_{10}-CCT GTA ATA AAC CCG AAA AT-3′).

in solution and not on a chip). In fact, only two general solution-based approaches have been taken. One involves the use of the intense surface plasmon resonance of DNA-functionalized gold nanoparticle probes and their aggregate size-dependent resonance shifts as indicators of DNA hybridization.[11] This approach offers a target sensitivity limit in the high picomolar (10^{-12}, pM) to low nanomolar (10^{-9}, nM) concentration range.[11] More recently, variants of it have been used to screen a variety of DNA binding molecules and enzyme inhibitors.[32−34] Another more sensitive approach uses the increased scattering efficiency of nanoparticles immobilized on a surface allowing for DNA detection at concentrations as low as 100 aM.[25,30,35] In this report, we present a new homogeneous detection method that uses gold nanoparticle probes in solution, as diagnostic surrogates for nucleic acid targets that is simple, quantitative, and inexpensive (Scheme 1). Solution-phase growth of the gold nanoparticle probes through electroless deposition of silver results in an increase of the particle size, which scales with light scattering efficiency.[36] The results of the assay can be measured and quantified with a UV−visible spectrometer and, in some cases, visually monitored with the unaided eye.

EXPERIMENTAL SECTION

Chemicals and Materials. Nanopure water (18 MΩ; Barnstead International) was used in all experiments and to prepare all buffers. All commercial reagents were used as received unless otherwise noted. The DNA strands were purchased from Integrated DNA Technologies, Inc. and were HPLC purified prior to use. Citrate-stabilized Au NP probes (13-nm diameter[37]) were prepared following standard literature procedures.[38] Magnetic microparticle probes (MMPs) were prepared from tosyl-activated magnetic beads (2.8 μm, concentration = 2×10^9 beads/mL, Dynal Biotech/Invitrogen Corp., Dynabeads M-280) using the manufacturer's protocol (3 μg of DNA was used to modify 10^7 particles).

Methods. In a typical experiment, 25 μL of prerinsed MMPs (5 mg/mL) and 25 μL of phosphate buffer saline (0.1 M NaCl in 0.01 M of sodium phosphate buffer, pH = 7, denoted PBS unless otherwise stated) were mixed in a 1.5-mL microcentrifuge tube (Ambion Inc., RNAse/DNAse free, nonstick). Following addition of 10 μL of nucleic acid target sample at designated concentrations over the 1 fM−10 nM concentration range, the solution was vigorously stirred at 37 °C (New Brunswick Scientific, Incubator I2400) for 30 min, with care not to allow settling of the magnetic microparticles. A bar magnet was used to magnetically attract the MMPs to the reaction sidewall, allowing for repeated washing with PBS (3×50 μL). The MMPs with captured target were redispersed in PBS (25 μL), and oligonucleotide-modified gold nanoparticle probes (Au NPs) were then added to the test solution (25 μL of 5 nM 13-nm-diameter particles). The solution was vigorously stirred at 37 °C for 30 min, in order to allow hybridization between the captured target, MMPs, and the Au NPs. The sandwich complexes were then magnetically separated and washed four times with 50 μL of PBS buffer. Water (100 μL) was added to the test solution, and the sample was vigorously stirred at 50 °C for 10 min allowing for full dehybridization of the Au NPs from the magnetic microparticles and target. A bar magnet was used to separate the free MMPs from the supernatant with the Au NPs.

Finally, silver amplification solution (40 μL, Ted Pella Inc.) was added to the collected supernatant, which resulted in silver deposition on the surface of the Au NPs, with a rate dependent on the Au NP concentration. Negative control samples were obtained from assays carried out in the absence of nucleic acid target. Immediately after the addition of the silver amplification solution, droplets (20 μL) of the reaction were pipetted onto a microscope slide (Fisherbrand, Frosted Microscope slides, precleaned) and positioned in the holder of a white light waveguide source (Fiber Lite, PL 750) for data acquisition. The scattering images of the droplets were captured at different times using a digital camera (Sony CyberShot DSC-W1, 5.1 Megapixel).

The hydrodynamic radius of the growing particles in solution was also investigated as a function of time using a dynamic light scattering instrument (Malvern Instruments, Zetasizer Nano ZS). The DLS sample consisted of 100 μL of gold nanoparticle probes (10 nM), 700 μL of water, and 200 μL of silver staining solution (final Au NP concentration 1 nM). The nanoparticles that were isolated following magnetic separation from the DNA assay (100 μL) were diluted to 500 μL with water, silver amplification solution (200 μL) was added, and UV−vis spectra were collected as a function of time. UV−vis spectra (Hewlett-Packard 8452a)

(32) Han, M. S.; Lytton-Jean, A. K. R.; Oh, B. K.; Heo, J.; Mirkin, C. A. *Angew. Chem., Int. Ed.* **2006**, *45*, 1807−1810.
(33) Han, M. S.; Lytton-Jean, A. K. R.; Mirkin, C. A. *J. Am. Chem. Soc.* **2006**, *128*, 4954−4955.
(34) Xu, X.; Han, M. S.; Mirkin, C. A. *Angew. Chem., Int. Ed.* **2007**, *46*, 3468−3470.
(35) Storhoff, J. J. M.; Sudhakar S.; Garimella, Viswanadham; Mirkin, Chad A. In *Microarray Technology and Its Applications*; Mueller, U. R. N., Dan V., Eds.; Springer GmbH: Berlin, Germany, 2005; pp 147−179.
(36) Sanedrin, R. G.; Georganopoulou, D. G.; Park, S.; Mirkin, C. A. *Adv. Mater.* **2005**, *17*, 1027−1031.
(37) Frens, G. *Nat. Phys. Sci.* **1973**, *241*, 20−22.
(38) Jin, R. C.; Wu, G. S.; Li, Z.; Mirkin, C. A.; Schatz, G. C. *J. Am. Chem. Soc.* **2003**, *125*, 1643−1654.

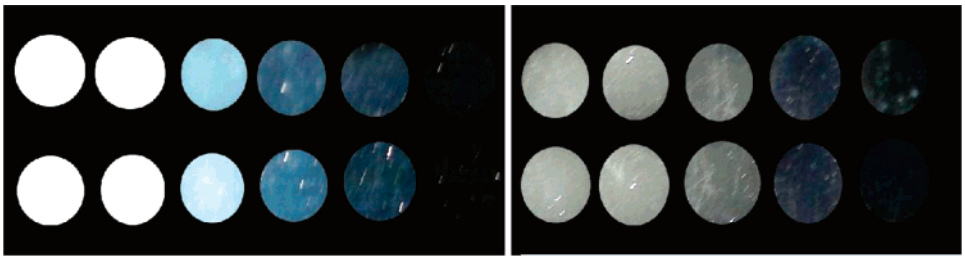

Figure 1. Optical images of droplets consisting of various initial Au nanoparticle concentrations that grew into larger particles following silver amplification. Images on the left were taken after 2 min of amplification, while images on the right were obtained after 10 min of amplification.

were also collected from standard diluted samples in addition to the Au NPs released in the assay in order to track extinction at 450 nm as a function of particle size.

An alternate, high-throughput method for carrying out the signal transduction involved pipetting the Au NP solutions (60 μL) into the wells of a microplate prior to silver enhancement (Corning Inc., 96 well 1/2 area, Costar). Simultaneous addition of 40 μL of the silver amplification solution to each well was carried out with the aid of a multichannel pipet (Fisher Scientific, Finnpipette II). The extinction at 450 nm from each well was followed as a function of time using an absorbance plate reader, until the solution in each well became opaque (Molecular Devices, SpectraMax 190). In addition, the silver amplification of 1 nM gold particles was followed in a 1-mL quartz cuvette using a UV−vis spectrophotometer. It should be noted that the two UV−vis experiments (Figure 3A/B) have not been standardized to a 1-cm path length.

Electron microscopy images of silver-deposited seeds were obtained with a Hitachi H-8100 TEM. Extinction spectra (used to calculate gold nanoparticle and nucleic acid concentrations) were recorded using a diode array spectrophotometer (Hewlett-Packard 8452a). The concentrations of DNA solutions and gold nanoparticle probes were calculated using Beer's law, with obtained extinction spectra, using the extinction coefficients for each strand (see: http://www.basic.northwestern.edu/biotools/OligoCalc.html) and 13-nm gold NPs ($\epsilon_{NP13}^{520nm} = 2.7 \times 10^8$), respectively.

Safety Considerations. To the best of our knowledge, this assay presents no serious hazards, though caution should be taken to avoid skin and eye contact with the silver enhancement solution. In addition, when the assays are used in conjunction with unknown biological samples, all proper government safety protocols should be followed.

RESULTS AND DISCUSSION

In a typical assay, DNA-modified magnetic microparticles were added to the sample solution in order to hybridize and capture DNA targets, Scheme 1. The captured DNA target−MMP complexes were isolated with a bar magnet, and nanoparticle probes complementary to a different region of the target were added. This resulted in the sandwiching of the DNA target between the magnetic and gold particle probes according to previously reported procedures.[39] Following target capture, the sandwich structures were isolated using a magnetic field and then washed with buffer to eliminate any unbound gold nanoparticle probes. Pure water was added to the reaction vessel (an Eppendorf tube) to resuspend the target−probe sandwich complexes, and the mixture was heated to 50 °C to facilitate dehybridization of the duplexes into their single-strand forms (the duplex maintains a high local salt concentration, due to the previous ionic conditions). A magnet was then used to separate the magnetic particles from the gold nanoparticle probes and target. Following dehybridization of the complexes, the number of nanoparticles was assumed to be equal to the number of target nucleic acid strands captured. This assumption is reasonable, since there is a substantial excess of capture sequences on the magnetic particles (10^{12}) as compared to the total number of targets (e.g., at 10 fM, there are $\sim 10^5$ target copies). Since there is an abundance of gold nanoparticle probes (8×10^{10}), the probability of a single gold particle sandwiching multiple targets is negligible. Finally, the colorimetric signature and light scattering capabilities of the gold nanoparticle probes were amplified by the addition of an Ag^+/hydroquinone solution, which results in the deposition of Ag^0 on the Au nanoparticle probes in solution. This deposition and growth process is easily monitored using a variety of techniques, including visual readout, UV−vis spectroscopy, and dynamic light scattering.

In order to optimize the assay, it was important to study the silver amplification of gold nanoparticle probes in solution under controlled conditions to evaluate how they might affect the dynamic range, detection limit, time, and readout of the assay. The scattering amplification can be qualitatively assessed with the naked eye by monitoring the conversion of the test solution from a transparent state to a cloudy gray color. At higher nanoparticle concentrations (greater than 1 nM), this appears as a red to gray transition because of the intense plasmon band of the dispersed gold nanoparticles at 520 nm. A more quantitative way to monitor the change in the scattering of the solutions is to pipet $\sim$10 μL of each particle suspension onto an unmodified microscope slide that can be used as a waveguide for white light. The degree of light scattering as determined by the color or intensity of the spot provides a quick and easy way to estimate the nanoparticle concentration (Figure 1). For example, at 100 pM Au NP concentration after 2 min of silver development, the solution appears pale blue. Above 100 pM, the solution concentrations become difficult to differentiate from each other as they are saturated and scatter white light. For nanoparticle concentrations below 100 pM, the solutions enhanced for 2 min appear as differing shades of blue. For some Au NP concentrations (<1 pM), 2-min amplification time is not sufficient to generate detectable

(39) Thaxton, C. S.; Hill, H. D.; Georganopoulou, D. G.; Stoeva, S. I.; Mirkin, C. A. *Anal. Chem.* **2005**, *77*, 8174−8178.

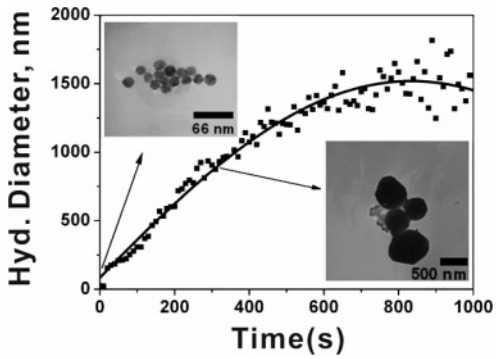

Figure 2. Dynamic light scattering results monitoring the growth of 13-nm Au nanoparticles after an excess of silver amplification solution was added to the solution.

scattering (Figure 1, left panel). However, if the reaction is allowed to proceed for 10 min, 1 pM, 100 fM, and 10 fM provide a scattering signal that can be easily differentiated with the naked eye from background (Figure 1 right panel). There are a couple of interesting assay readout features that depend upon amplification time worth noting. For the assay with 2-min amplification times, there are intensity differences depending upon initial nanoparticle concentration. At higher particle concentrations (1−10 nM), amplification results in a collection of particles that scatter white light (leftmost region, left panel, Figure 1). This is a false color effect from the camera due to an extended exposure time. With the naked eye, solutions at high concentrations appear bright blue/gray. At intermediate and lower concentrations, the scattering appears blue to the naked eye. In order to observe particle concentrations below 1 pM, 10-min amplification times were required. Interestingly, in this concentration range, the particles must grow considerably larger before they scatter enough light to be observed with the naked eye. This method allows for an estimation of target concentration based upon color that can be discerned with the naked eye.

To prove that the gold nanoparticles were indeed growing in size, the hydrodynamic radius of the Au NPs was monitored by DLS. The data show that upon addition of the silver amplification solution the hydrodynamic radius of the particle changes from ~18 to ~40 nm (Figure 2). This process occurs over the first few seconds of the amplification step. The particles keep growing over a 10-min period until they are ~0.7 μm in diameter. The particle sizes were independently confirmed by TEM (insets, Figure 2). Under these conditions, the readout method has limited use with particles larger than ~0.7 μm due to limitations of the DLS instrument, interference from the large particles that render the solution opaque, and particle instability making DLS poorly suited for quantification.

For applications requiring rigorous quantification, UV−vis spectroscopy can be used to measure the relative extinction intensities of the amplified particles. To evaluate the quantitative capabilities of this detection system, we studied solutions that spanned the 10 nM−1 fM concentration range (Figure 3A). The UV−vis spectra show that the plasmon band for the 13-nm Au nanoparticles (spectrum 1) disappears almost immediately upon addition of the Ag amplification solution. The resulting silver-coated gold nanoparticles continue to grow, with a characteristic band at 450 nm increasing in intensity and broadening, in part, due to particle light scattering.[40,41]

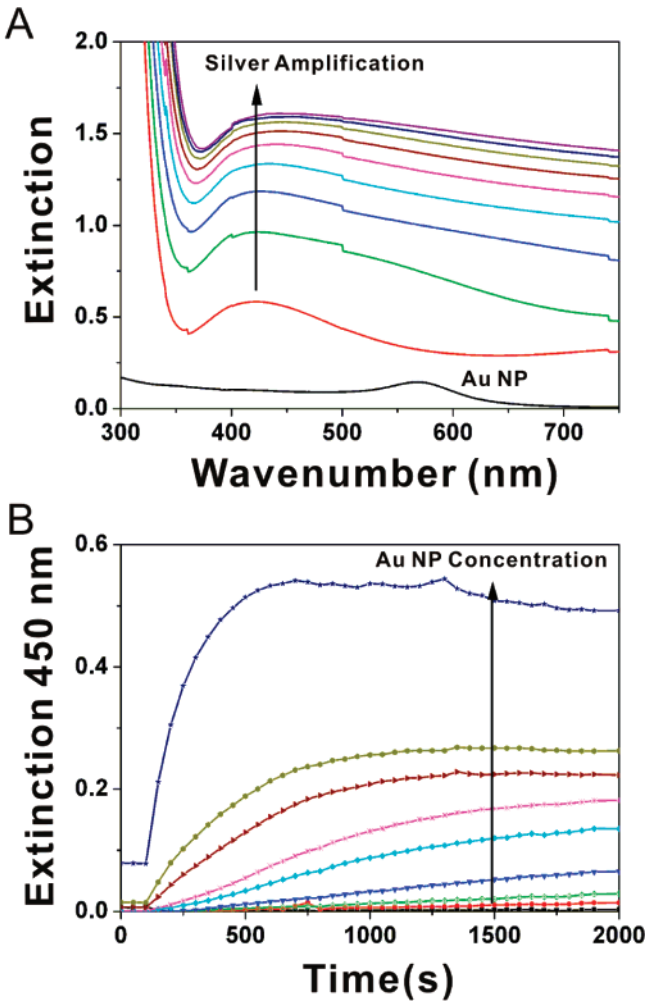

Figure 3. (A) Extinction spectra following the growth of Au NPs. (B) Plot of extinction intensity at 450 nm as a function of time for various initial concentrations of Au nanoparticles. Note: the decreasing intensity at the highest Au NP concentration, postamplification, is due to particle settling. The concentrations shown above are (top to bottom: 10 nM, 1 nM, 100 pM, 10 pM, 1 pM, 100 fM, 10 fM, no particles).

Interestingly, a dilution series of the Au nanoparticles spanning the range from 10 nM to 1 fM shows that the rate of particle growth is highly dependent on the initial particle concentration (Figure 3B). The extinction maximum at 450 nm in the spectrum for the different nanoparticle concentrations levels off at different intensities and over different time scales. By UV−vis spectroscopy, the maximum extinction values are attained as soon as 8 min after the addition of the silver amplification solution for a 10 nM solution of Au NPs and as long as 30 min for a 10 fM solution of particles. An innovative aspect of this method is the use of maximum extinction to quantitatively detect Au NPs at concentrations as low as 10 fM. One can simply look at the spectra in Figure 3B and see that the end points as determined by extinction leveling are quantitative indicators of particle concentration.

After gaining an understanding of the kinetics of silver enhancement, particle limits of detection (LODs), and readout

(40) Morriss, R. H.; Collins, L. F. *J. Chem. Phys.* **1964**, *41*, 3357−3363.
(41) Rivas, L.; Sanchez-Cortes, S.; Garcia-Ramos, J. V.; Morcillo, G. *Langmuir* **2000**, *16*, 9722−9728.

options, we evaluated the assay in the context of DNA detection. A dilution series of nucleic acid targets, comprising sequence sections that were identified as conserved areas of the HIV-2 virus, were isolated and analyzed following Scheme 1 and as described above. An amplification time of 30 min was employed to obtain maximum extinction intensities from each sample (Figure 4). Under these conditions, the assay has an LOD of 10 fM and a linear range from high femtomolar to low nanomolar. To detect unknown target concentrations with this method, a standard curve (a general research tool for quantitative analysis of unknown concentrations) would need to be used. Though this detection method is not as sensitive as the recently developed bio-barcode assay[39,42−44] due to the lack of the amplification step resulting from the oligonucleotide substitution for the initial target, it does have some highly significant and useful attributes. It has a convenient colorimetric readout, is highly reproducible and rapid, does not require microarray components (which lowers the total cost substantially), and exhibits a sensitivity great enough for various applications where PCR would not be necessary.[45−47]

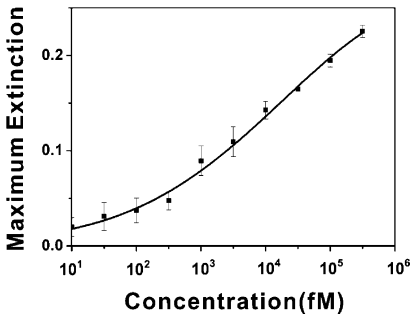

Figure 4. Detection results for DNA target concentrations in the 10 fM−1 nM range.

CONCLUSIONS

A novel way of quantitatively detecting nucleic acids has been developed. The method is straightforward to implement and offers an LOD of 10 fM. Importantly, it can be read out qualitatively with the naked eye or quantitatively with a low-cost absorbance device. These attributes make the technology very attractive for mobile and point-of-care uses.[19,35,48,49] Significantly, in principle, the concept can be easily extended to other analytes such as proteins, certain metal ions, and small molecules that can be sandwiched with gold nanoparticle probes modified with the appropriate recognition agents.[50,51,52] Efforts in this direction are underway.

ACKNOWLEDGMENT

The authors thank Fengwei Huo for his assistance with Transmission Electron Microscopy. C.A.M. acknowledges AFOSR, DARPA, NCI, NSF, and The Doris Duke Foundation for generous support of this work. He is also grateful for a NIH Director's Pioneer Award. H.D.H. acknowledges the U.S. Department of Homeland Security (DHS) for a Graduate Fellowship under the DHS Scholarship and Fellowship Program.

Received for review April 27, 2007. Accepted June 13, 2007.

AC070867G

(42) Nam, J. M.; Park, S. J.; Mirkin, C. A. *J. Am. Chem. Soc.* **2002**, *124*, 3820−3821.
(43) Nam, J. M.; Stoeva, S. I.; Mirkin, C. A. *J. Am. Chem. Soc.* **2004**, *126*, 5932−5933.
(44) Georganopoulou, D. G.; Chang, L.; Nam, J. M.; Thaxton, C. S.; Mufson, E. J.; Klein, W. L.; Mirkin, C. A. *Proc. Natl. Acad. Sci. U.S.A.* **2005**, *102*, 2273−2276.
(45) Lanciotti, R. S.; Kerst, A. J.; Nasci, R. S.; Godsey, M. S.; Mitchell, C. J.; Savage, H. M.; Komar, N.; Panella, N. A.; Allen, B. C.; Volpe, K. E.; Davis, B. S.; Roehrig, J. T. *J. Clin. Microbiol.* **2000**, *38*, 4066−4071.
(46) Wang, J.; Rivas, G.; Cai, X.; Palecek, E.; Nielsen, P.; Shiraishi, H.; Dontha, N.; Luo, D.; Parrado, C.; Chicharro, M.; Farias, P. A. M.; Valera, F. S.; Grant, D. H.; Ozsoz, M.; Flair, M. N. *Anal. Chim. Acta* **1997**, *347*, 1−8.
(47) Jianrong, C.; Yuqing, M.; Nongyue, H.; Xiaohua, W.; Sijiao, L. *Biotechnol. Adv.* **2004**, *22*, 505−518.
(48) Thaxton, C. S.; Rosi, N. L.; Mirkin, C. A. *MRS Bull.* **2005**, *30*, 376−380.
(49) Goluch, E. D.; Nam, J. M.; Georganopoulou, D. G.; Chiesl, T. N.; Shaikh, K. A.; Ryu, K. S.; Barron, A. E.; Mirkin, C. A.; Liu, C. *Lab Chip* **2006**, *6*, 1293−1299.
(50) Stoeva, S. I.; Lee, J. S.; Smith, J. E.; Rosen, S. T.; Mirkin, C. A. *J. Am. Chem. Soc.* **2006**, *128*, 8378−8379.
(51) Chang, M. M. C.; Cuda, G.; Bunimovich, Y. L.; Gaspari, M.; Heath, J. R.; Hill, H. D.; Mirkin, C. A.; Nijdam, A. J.; Terracciano, R.; Thundat, T.; Ferrari, M. *Curr. Opin. Chem. Biol.* **2006**, *10*, 11−19.
(52) Huang, C. C.; Huang, Y. F.; Cao, Z. H.; Tan, W. H.; Chang, H. T. *Anal. Chem.* **2005**, *77*, 5735−5741.